Interface structure and thermal stability of epitaxial $SrTiO_3$ thin films on Si (001)

L. V. Goncharova[a] and D. G. Starodub
Department of Physics and Astronomy, and Laboratory for Surface Modification, Rutgers University, Piscataway, New Jersey 08854

E. Garfunkel
Department of Chemistry and Chemical Biology, and Laboratory for Surface Modification, Rutgers University, Piscataway, New Jersey 08854

T. Gustafsson
Department of Physics and Astronomy, and Laboratory for Surface Modification, Rutgers University, Piscataway, New Jersey 08854

V. Vaithyanathan, J. Lettieri, and D. G. Schlom
Department of Material Science and Engineering, The Pennsylvania State University, University Park, Pennsylvania 16802

(Received 9 January 2006; accepted 9 March 2006; published online 14 July 2006)

We have used medium energy ion scattering, temperature programmed desorption, and atomic force microscopy to study the interface composition and thermal stability of epitaxial strontium titanate thin films grown by molecular-beam epitaxy on Si (001). The composition of the interface between the film and the substrate was found to be very sensitive to the recrystallization temperature used during growth, varying from a strontium silicate phase when the recrystallization temperature is low to a Ti-rich phase for a higher recrystallization temperature. The films are stable towards annealing in vacuum up to ~550 °C, where SrO desorption begins and the initially flat film starts to roughen. Significant film disintegration occurs at 850 °C, and is accompanied by SiO and SrO desorption, pinhole formation, and finally titanium diffusion into the silicon bulk. © *2006 American Institute of Physics*. [DOI: 10.1063/1.2206710]

I. INTRODUCTION

It is only recently that relatively defect-free epitaxial oxide films have been successfully grown on silicon, with particular attention focused on the perovskite strontium titanate ($SrTiO_3$).[1–7] Contemporary interest has focused on the use of this class of epitaxial oxides as high-κ gate dielectrics because of its potential of providing a higher uniformity, lower defect density, lower leakage current alternative to polycrystalline metal oxides, or amorphous SiO_2 films. Moreover, excellent electrical properties of the $SrTiO_3$/Si stacks were reported with capacitance electrically equivalent to that of an SiO_2 film less than 10 Å thick.[1,2,4] Subsequent theoretical[8,9] and experimental[10] estimates of conduction band offsets have raised serious questions about the possibility of using $SrTiO_3$ as a substitute for SiO_2 in transistors. Another reason for interest in epitaxial $SrTiO_3$ is its potential use as a thin buffer layer, as its lattice structure permits epitaxial integration of other functional transition metal oxides into heterostructures.[11–17] Such structures would enable the integration of a range of oxides with silicon or germanium. As a result, significant effort has been made in growing "single crystal" $SrTiO_3$ films with ideal interface properties.[1,3–7,18] Although epitaxial structures of $SrTiO_3$ on silicon show less than 2% lattice mismatch, the two materials are intrinsically thermodynamically unstable next to each other, with some reduction of the $SrTiO_3$ and oxidation of the silicon expected.[19] Thus, any ideal epitaxial $SrTiO_3$/Si structures are metastable at best, and the kinetic properties of the growth and postprocessing will be of central importance.

Several different models have been proposed to describe the interfacial structure between epitaxial $SrTiO_3$ and the underlying silicon it is grown upon. These include amorphous SiO_2 interfaces,[3,18] reduced amorphous silicon oxide, or amorphous or crystalline (depending on the temperature) silicates,[20] crystalline monolayers consisting of strontium, silicon, and likely oxygen,[9,21] $Sr_{1-x}Ba_xO/SrSi_2$ layers,[1,4] etc. These models were based on x-ray photoemission spectroscopy (XPS) and/or high-resolution transmission electron microscopy (HRTEM) measurements, or were postulated from considering the initial growth sequence. Two crucial issues need to be addressed to better understand these systems. First, as film growth involves recrystallization at elevated temperatures,[1,5,7,22] it is not obvious that the final structure is that of the initial growth sequence. Second, and related, is how does the elemental composition of the interface and epitaxial film itself change during annealing treatments that might be used in the semiconductor industry (postdeposition reducing, oxidizing, or dopant-activation anneals).[1,23] So far only a limited number of studies have addressed these questions. Using Rutherford backscattering spectroscopy (RBS), nuclear reaction analysis, and XPS, Shutthanandan *et al.*[24] investigated the evolution of 20–1000 Å thick $SrTiO_3$ films on silicon. Growth of interfacial SiO_2 layers was found both

[a]Electronic mail: lgoncha@physics.rutgers.edu

in the case of annealing in ultrahigh vacuum (UHV) and in O_2. They concluded that the oxygen atoms removed from the $SrTiO_3$ film most probably migrated to the interface and are responsible for the formation or growth of interfacial SiO_x layers. A detailed study of the interface structure was not possible due to the lack of depth resolution in RBS ($\sim$100 Å).[25]

The aim of our work is to examine the structure and composition at the interface between epitaxial $SrTiO_3$ and silicon using a high-resolution elemental depth profiling technique—medium energy ion scattering (MEIS). We show how the initial structure and composition of the interface as well as additional postgrowth annealing affects the final structure and composition of the multilayer stack. We find that the structural integrity of the $SrTiO_3$ film can be maintained over a wide range of conditions or even improved, although heating to temperatures above 900 °C inevitably leads to degradation and eventually to full decomposition.

II. EXPERIMENT

Epitaxial $SrTiO_3$ films on Si (001) were grown by molecular-beam epitaxy (MBE) system (EPI 930) modified for the growth of oxides on silicon.[26] A quartz crystal microbalance was used to measure the fluxes of the elemental species to be deposited and *in situ* reflection high-energy electron diffraction (RHEED) was used to monitor the growth of the oxide film. Molecular beams of strontium (flux $J_{Sr} \sim 3\times10^{13}$ at./cm^2 s) from a conventional effusion cell, titanium (flux $J_{Ti} \sim 4\times10^{13}$ at./cm^2 s) supplied by a titanium sublimation pump (Ti-Ball),[27] and molecular oxygen were used as the elemental sources for $SrTiO_3$ deposition. The base pressure in the growth chamber was $\sim2\times10^{-9}$ Torr. The substrates were 50 mm diameter epiready commercial Si (001) wafers cut with an accuracy of ±0.1°. Prior to loading the silicon substrates into the MBE system, the surface organics were removed by ozone cleaning for 20 min.

The growth process is described in detail elsewhere,[5,22] but in brief it consisted of the following steps. A SiO_2-free silicon surface, identified by a sharp double-domain 2×1 Si (001) RHEED pattern, was obtained by heating in UHV to $\sim$980 °C. Upon the clean Si (001) surface at a substrate temperature of 700 °C (measured by an optical pyrometer), a strontium dose of 3.4×10^{14} at./cm^2 [1/2 ML (monolayer)[28] of strontium] was deposited from a strontium MBE source. This formed an interfacial strontium silicide layer[1,4] that functions to protect the underlying silicon from oxidation and thus preserve an epitaxial template for epitaxial oxide overgrowth.[29]

The wafer was then cooled to near room temperature (under 200 °C), where in UHV an additional 1/2 ML (3.4×10^{14} at./cm^2) of strontium was deposited. Unlike the strontium deposited at high temperature, which forms strontium silicide,[1,4] this strontium deposited at low temperature remains metallic and enables moving a little farther away from the interface before exposing the wafer to oxygen. This helps to avoid oxidizing the underlying silicon.

With the substrate still near room temperature (under 200 °C), oxygen was then introduced to a background pressure of 4×10^{-8} Torr and additional strontium was deposited in the presence of the oxygen to form a total of 3 ML of epitaxial SrO. The 1/2 ML of metallic strontium deposited prior to the oxygen exposure also gets oxidized during this step and becomes an integral part of the epitaxial SrO on silicon. The thickness of the epitaxial SrO layer on silicon is limited to its critical thickness value of $\sim$3 ML (based on observations of the RHEED patterns), due to the 5% lattice mismatch between SrO and silicon. On top of the 3 ML of crystalline SrO, 2 ML of amorphous TiO_2 was deposited in an oxygen background pressure of 3×10^{-7} Torr, with the substrate temperature still near room temperature (under 200 °C).

The oxygen was then turned off and the heterostructure was annealed in UHV at $\sim$450–550 °C to recrystallize a $SrTiO_3$ layer 2.5 unit cells thick through a topotactic reaction between the TiO_2 and the underlying SrO. In this topotactic reaction the TiO_2 diffuses into the crystalline SrO layer, transforming it into $SrTiO_3$, while maintaining its orientation relationship with the underlying silicon substrate.[22] The extent of diffusion of TiO_2 into the underlying SrO stack during the recrystallization depends on the recrystallization temperature and time. At $\sim$450 °C the recrystallization time is $\sim$1 h; at 550 °C it is $\sim$30 min. The intensity of the specular spot (along the [100] $SrTiO_3$ or equivalently [110] Si azimuth) and the half-order signature of a SrO-rich surface atop $SrTiO_3$ in the RHEED pattern (along the [110] $SrTiO_3$ or equivalently [100] Si azimuth)[30] during the recrystallization were used to qualitatively monitor the extent of TiO_2 indiffusion. These observations are confirmed by the MEIS measurements described in this paper.

Further growth of the epitaxial $SrTiO_3$ layer to the desired film thickness was achieved on this recrystallized 2.5 unit-cell-thick $SrTiO_3$ template layer through the repeated codeposition (Sr+Ti+O_2 molecular beams) of an amorphous $SrTiO_3$ layer near room temperature (under 200 °C), followed by recrystallization at $\sim$450–550 °C in UHV. Such film growth is analogous to the "periodic annealing" method developed by Cho[31] to grow GaAs by MBE. Based on *in situ* RHEED and *ex situ* x-ray characterization, it was found that the smooth and relatively high structural quality epitaxial $SrTiO_3$ films were obtained when the $SrTiO_3$ deposited and recrystallized in each step was three to five unit cells thick.[22]

The annealing experiments were carried out in two different ultrahigh (UHV) chambers. Films were annealed in the main scattering MEIS chamber (base pressure $<3\times10^{-10}$ mbar) followed by MEIS measurements. Prior to MEIS analyses all the samples were degassed thoroughly at $T<300$ °C. The temperature was measured by an optical pyrometer calibrated with a thermocouple. Thermal desorption spectroscopy (TDS) data were acquired using an Inficon Quadrex 200 quadrupole mass spectrometer. An additional aperture was installed between the sample and the ionization region to insure that only the central part of the heated sample was in direct line of sight with the mass spectrometer.

MEIS is a low energy, high-resolution version of conventional Rutherford backscattering. By using an electrostatic ion energy analyzer,[32,33] it is possible to obtain subna-

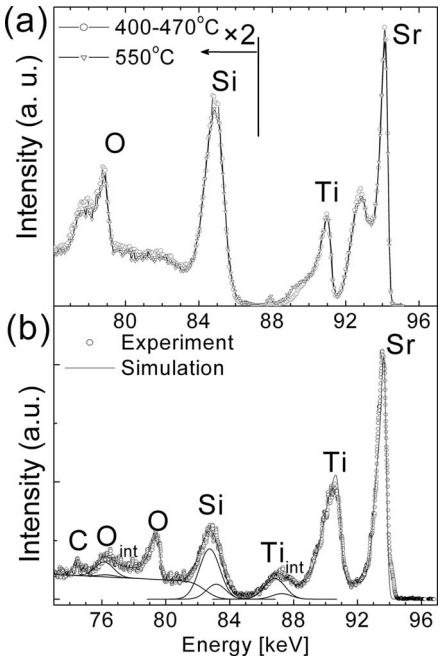

FIG. 1. MEIS energy distributions for (a) 35 Å thick $SrTiO_3$ films on Si (001) recrystallized at 450 and 550 °C, and (b) a 78 Å thick $SrTiO_3$ film recrystallized at 550 °C. Interface peak deconvolution is demonstrated for a thicker film.

nometer depth resolution. The experiments were performed using 98–130 keV H^+ beams. Analysis of the top surface termination was done in a double aligned geometry in the (110) scattering plane, in which the incoming beam was aligned with the $SrTiO_3$ film $[\bar{1}1\bar{1}]$ channeling direction, and the detector axis with the $[\bar{1}11]$ film crystallographic axis. For the depth profile analysis, the incident beam was aligned normal to the surface and the backscattered ions were detected along the [011] direction of the $SrTiO_3$ film. To ascertain the difference in ion straggling between channeling and random directions, additional measurements were conducted at ~10° off axis. The MEIS beam size at the sample was $\sim 1 \times 0.1$ mm^2; the spectra cannot give direct information about possible lateral inhomogeneities in the sample on a scale smaller than the beam size.

Ex situ atomic force microscope (AFM) measurements under ambient conditions were carried out using a JEOL JSPM 4210 in the "tapping" mode.

III. RESULTS

MEIS depth profiles for 35 Å thick (nine unit cells) $SrTiO_3$ films recrystallized at 450 and 550 °C are presented in Fig. 1(a). The degree of crystallinity of the films is determined by taking the ratio of the yield in the channeling geometry to a (calculated) random direction yield ("the maximum yield"). These ratios for thicker films (>70 Å), where the signals from a film's surface, bulk, and interface are well separated, range from 1% to 4%, thus the films appear to be quite well ordered. Distinct peaks of strontium, titanium, and oxygen can be observed corresponding to the top surface layer of the $SrTiO_3$ film. In addition, interface peaks of the same elements are also observed slightly lower in energy.

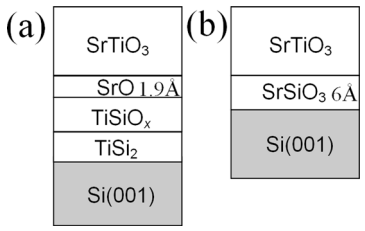

FIG. 2. Interface compositions for $SrTiO_3$ films recrystallized at (a) 550 °C and (b) 400 °C. Note that interface becomes enriched with titanium as the recrystallization temperature increases.

As we are using a channeling and blocking configuration, we do not detect subsurface atoms in lattice positions. Atoms in an amorphous region of the sample, however, or those in a crystalline region, but in positions that are situated away from the rows of atoms positioned "above" them in the film, will be visible to the ion beam. Furthermore, due to the proton energy loss inside the film the scattering from interface species will likely be separated from the surface signal. Figure 1(b) presents the results for a somewhat thicker (78 Å) $SrTiO_3$ film (recrystallized at 550 °C), where the separation between surface and interface peaks is correspondingly larger.

Quantitatively, the spectrum in Fig. 1(b) can be modeled by a ~78 Å crystalline $SrTiO_3$ film on top of a ~2 Å partially visible SrO layer, a $TiSi_xO_y$ layer, and a $TiSi_x$ layer or islands extending deeper into bulk silicon [Fig. 2(a)]. This composition clearly deviates from the initial deposition sequence: the first and crucial step in the film growth involves depositing a small number of strontium atoms on the substrate,[4,26] forming a Sr enriched interface. The fractional (0.4–0.7) number of atoms visible to the ion beam in the interfacial region indicates that the interfacial layer is crystalline.

Perovskite $SrTiO_3$ structures can be considered as consisting of alternating SrO and TiO_2 layers. MEIS measurements in the (110) $SrTiO_3$ scattering plane allow us to determine the surface termination. If the incident beam is aligned with the [111] $SrTiO_3$ direction (54.74° off normal) and the detector is positioned along the $[1\bar{1}\bar{1}]$ axis, two distinct situations are possible. If the top surface is a SrO layer [Fig. 3(a), SrO termination], every titanium atom in the second layer will be within the shadow cone of a strontium atom and the measured titanium yield will be much smaller than that of strontium. Calculated angular distributions for strontium and titanium assuming such a SrO termination are shown in Fig. 3(a). For the semiquantitative analysis we assume the bulk terminated surface. The other alternative is TiO_2 termination, where every strontium atom is shadowed by a titanium atom. The simulated ion yields for this case are presented in Fig. 3(b). The simulations clearly imply that the surface is predominantly SrO terminated. A numerically better fit is obtained by assuming ~80% SrO and 20% TiO_2 termination [Fig. 3(c)]. We conclude that the surface is predominately SrO terminated. The SrO termination is also confirmed by measuring the energy shifts between leading edges of Sr and Ti peaks in the energy spectra.

Control over the interfacial region composition can be

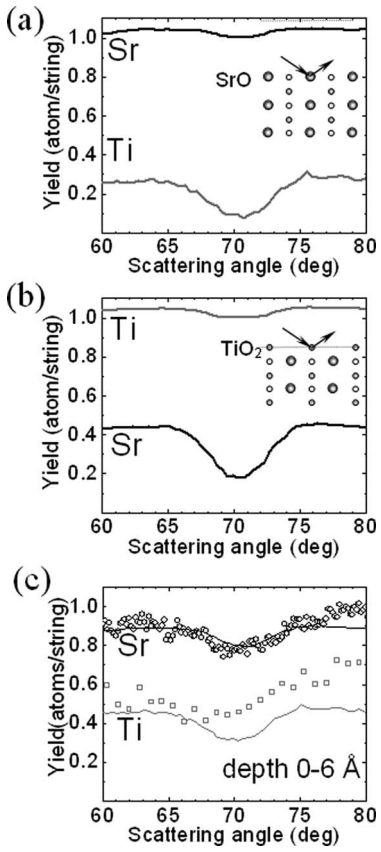

FIG. 3. Angular distributions of the backscattered ions corresponding to Sr and Ti peak integrated intensities. Simulation curves are shown for a SrO terminated film in (a) and a TiO_2 terminated film in (b), whereas experimental results with the best fit simulated data are presented in (c).

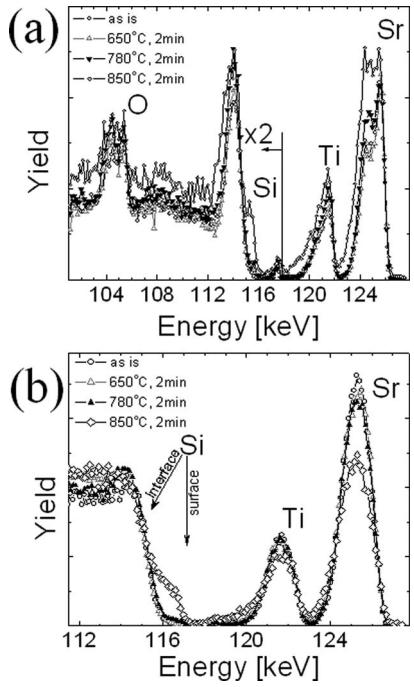

FIG. 4. MEIS spectra for a 35 Å thick $SrTiO_3$ film recrystallized at 400 °C and annealed to $T=650-850$ °C for 2 min consequently. (a) Channeling and (b) random directions data are shown.

achieved by carefully varying the recrystallization temperature during growth. By comparing the area of the interface peaks, we conclude that the number of strontium and titanium atoms detected in this region (aligned away from ideal overlayer lattice sites) is approximately the same, and slightly smaller than that of oxygen. For high recrystallization temperatures, the titanium interface peak extends to lower energy, most likely indicating $TiSi_x$ formation. $TiSi_2$ precipitates have been identified by HRTEM studies on similar $SrTiO_3$/Si (001) films prepared using an ~550 °C recrystallization temperature.[34] The data for the film recrystallized at 450 °C [Fig. 1(a)] show a narrower titanium peak, indicating that in this case titanium is not moving deeper into the substrate. The interface composition can be modeled as a $SrSi_xO_y$ crystalline layer for this sample [Fig. 2(b)].

After heating the low recrystallization temperature sample in vacuum, the sample composition and structure changes gradually (Fig. 4). At 650 °C, there is first an improvement of the film crystallinity, as indicated by a small reduction of the titanium interface peak. After annealing to 780 °C we see an increase in the strontium, silicon, and oxygen interface peaks, indicative of the onset of disorder of the strontium and oxygen sublattices, or alternatively an increase in the interfacial $Sr-Si-O_x$ layer at this temperature.

There are no significant changes at higher temperatures until partial film disintegration starts at 850 °C. The Sr peak area as well as yields of other elements (Ti, Si, and O) increase in channeling geometry. Whereas the reduction of the Sr peak area in the random geometry assumes removal of Sr into the gas phase, presumably in the form of SrO. Above 850 °C, we observe an onset of titanium diffusion into the silicon bulk, accompanied by the appearance of a surface silicon peak in both channeling and random geometries. This shows that silicon atoms now exist at the surface and implies the appearance of lateral discontinuities or/and silicate formation in the film. $SrTiO_3$ film decomposition is complete at 950 °C, where only titanium and silicon surface peaks are observed (not shown).

The decomposition process occurring during film annealing in vacuum was monitored using TDS in the temperature range of RT-1000 °C (Fig. 5). Several mass channels were monitored simultaneously corresponding to O ($m=16$), O_2 ($m=32$), SiO or CO_2 ($m=44$), Ti ($m=48$), Sr ($m=88$), and SrO ($m=104$) desorption species. The only volatile form of strontium and titanium found to desorb was SrO, starting at ~500 °C. The amount of desorbed material is relatively small, possibly representing the decomposition of surface layers only. The bulk decomposition of $SrTiO_3$ starts at ~900 °C as indicated by the loss of oxygen-, silicon-, and strontium-containing species from the surface, implying the complete decomposition of the film.

An AFM image of the surface topography of the as-grown film [Fig. 6(a)] shows flat terraces with neither detectable roughness nor signs of microvoids or grains. After annealing to the highest temperatures, a fraction of the surface is covered with 50–100 Å high islands [Fig. 6(b)]. According to MEIS these islands are titanium silicide, presumably partially oxidized after exposure to air.

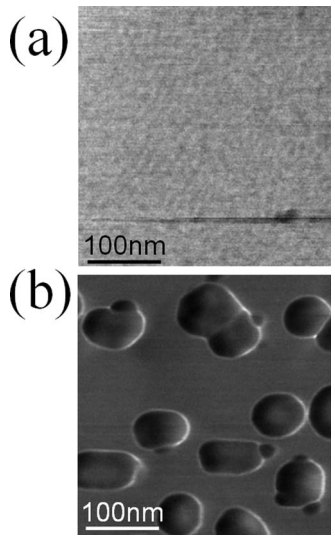

FIG. 5. AFM images (300×300 nm^2) of the $SrTiO_3$ surface depending on annealing temperature: (a) before annealing and (b) after annealing to 950 °C.

IV. DISCUSSION

Our results indicate that high quality epitaxial $SrTiO_3$ film growth can be achieved with a very thin $Sr-SiO_x$ interfacial layer. For higher recrystallization temperatures we observe the formation of a titanium silicide phase in the interfacial region, which would likely be detrimental for most device applications. There is still debate about what the composition and interface structure of an ideal $SrTiO_3/Si$ heterojunction should be. For certain applications, a very thin low-κ (SiO_2 or silicate) layer may actually be desirable to (i) passivate the interface (minimizing the number of interface trap states), (ii) change the band alignment (epitaxial $SrTiO_3/Si$ is thought to have a very low offset),[8–10] and/or (iii) relieve strain in the system.

Our results show that the initial films are crystalline with a flat surface. Low temperature annealing (<650 °C) causes minor surface disordering associated with some SrO loss and desorption of the carbon-containing species. In MEIS we see carbon loss (the carbon peak disappears) and the top surface layer changes from predominantly SrO termination to TiO_2 termination. SrO desorption was also observed by Shin *et al.*[35] in epitaxial $SrRuO_3/SrTiO_3$ (001) films with a desorption peak at ~480 °C. The surface stability of epitaxial $SrRuO_3/SrTiO_3$ (001) noted above is also strongly affected by the presence of surface contaminants after air exposure.[35] In our work we do not see significant differences in the total number of oxygen atoms before and after annealing within experimental uncertainties.

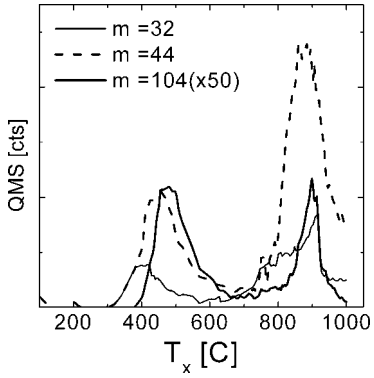

FIG. 6. Temperature desorption spectra for a 35 Å thick $SrTiO_3$ film on Si (001) recorded for selected mass channels and a heating rate of 1.5 K s^{-1}.

The appearance of a surface silicon peak after annealing >850 °C indicates that the continuity of the $SrTiO_3$ film was broken. Formation of pinholes was also observed as an intermediate step during the annealing of other high-κ/Si systems [HfO_2,[23] Al_2O_3 (Ref. 36)]. More intriguing is that the strontium and titanium peak widths broaden at the same time. Two mechanisms might account for this effect. The first possibility is a chemical reaction between the $SrTiO_3$ film and the silicon substrate (expected based on thermodynamics),[19] which would result in a thicker intermixed interfacial layer. The less likely second scenario is a partial $SrTiO_3$ phase separation into a mixture of SrO and TiO_2 as an intermediate step, which could produce oxide islands with varying heights and may expose the silicon substrate. We directly observe the desorption of SrO ($m=104$), SiO ($m=44$), and O_2 ($m=32$) in TDS data. Therefore, the overall process can be described by the equation,

$$SrTiO_3 + 3Si \rightarrow SiO(g)\uparrow + SrO(g)\uparrow + \tfrac{1}{2}O_2(g)\uparrow + TiSi_2.$$

The HRTEM study[34] also indicate that some of the as-grown $SrTiO_3/Si$ samples that were recrystallized at higher temperature form interfacial $TiSi_2$, with no evidence for the TiO_x formation. On the other hand grazing incidence x-ray diffraction (GIXRD) studies of polycrystalline $SrTiO_3$ films deposited on Si (111) (Ref. 37) show evidence for the $SrTiO_3$ phase separating into SrO and TiO_x oxides after rapid thermal annealing (RTA) to temperatures >850 °C. Hence the possibility of $SrTiO_3$ decomposition with the formation of SrO and TiO_x phases cannot be completely excluded.

V. CONCLUSIONS

In summary, the interface between MBE-grown epitaxial $SrTiO_3$ and silicon was studied using MEIS. A crystalline $Sr-Si-O_x$ interface was demonstrated for samples recrystallized at 450–475 °C. Higher recrystallization temperatures resulted in titanium diffusion into the silicon substrate with most likely $TiSi_x$ islands forming at the interface. The films were found to be quite stable under annealing in vacuum at $T<750$ °C; above that temperature atomic disordering of the strontium, titanium, and oxygen sublattices starts. Upon annealing to 850 °C or higher, film decomposition occurs, accompanied by SrO and SiO desorption, pinhole formation, and finally diffusion of titanium into the silicon bulk.

ACKNOWLEDGMENTS

The authors would like to acknowledge financial support from the SRC/Sematech FEP Center, NSF (DMR 0218406), and the Office of Naval Research through contract N00014-04-1-0426. The authors also would like to thank Weirong Jiang for the AFM measurements.

[1]S. Jeon, F. J. Walker, C. A. Billman, R. A. McKee, and H. Hwang, IEEE Electron Device Lett. **24**, 218 (2003).
[2]K. Eisenbeiser *et al.*, Appl. Phys. Lett. **76**, 1324 (2000).
[3]Z. Yu, J. Ramdani, J. A. Curless, J. M. Finder, C. D. Overgaard, R. Droopad, K. W. Eisenbeiser, J. A. Hallmark, and W. J. Ooms, J. Vac. Sci. Technol. B **18**, 1653 (2000).
[4]R. A. McKee, F. J. Walker, and M. F. Chisholm, Phys. Rev. Lett. **81**, 3014 (1998).
[5]J. Lettieri, Ph.D. thesis, Pennsylvania State University, 2002. Available online at http://etda.libraries.psu.edu/theses/approved/WorldWideIndex/ETD-202/index.html
[6]H. Li *et al.*, J. Appl. Phys. **93**, 4521 (2003).
[7]F. J. Walker and R. A. McKee, in *High Dielectric Constant Materials: VLSI MOSFET Applications*, edited by H. R. Huff and D. C. Gilmer (Springer, Berlin, 2005), pp. 607–637.
[8]J. Robertson and C. W. Chen, Appl. Phys. Lett. **74**, 1168 (1999).
[9]X. Zhang, A. A. Demkov, H. Li, X. Hu, Y. Wei, and J. Kulik, Phys. Rev. B **68**, 125323 (2003).
[10]S. A. Chambers, Y. Liang, Z. Yu, R. Droopad, J. Ramdani, and K. Eisenbeiser, Appl. Phys. Lett. **77**, 1662 (2000).
[11]A. C. Tuan, T. C. Kaspar, T. Droubay, J. W. Rogers, and S. A. Chambers, Appl. Phys. Lett. **83**, 3734 (2003).
[12]E. Tokumitsu, K. Itani, B.-K. Moon, and H. Ishiwara, Jpn. J. Appl. Phys., Part 1 **34**, 5202 (1995).
[13]A. Lin, X. Hong, V. Wood, A. A. Verevkin, C. H. Ahn, R. A. McKee, F. J. Walker, and E. D. Specht, Appl. Phys. Lett. **78**, 2034 (2001).
[14]Y. Wang *et al.*, Appl. Phys. Lett. **80**, 97 (2002).
[15]B. T. Liu *et al.*, Appl. Phys. Lett. **80**, 4801 (2002).
[16]A. Goyal, M. P. Paranthaman, and U. Schoop, MRS Bull. **29**, 552 (2004).
[17]J. Junquera and P. Ghosez, Nature (London) **422**, 506 (2003).
[18]Z. Yu *et al.*, Mater. Res. Soc. Symp. Proc. **747**, T3.1.1 (2003).
[19]K. J. Hubbard and D. G. Schlom, J. Mater. Res. **11**, 2757 (1996).
[20]X. Hu *et al.*, Appl. Phys. Lett. **82**, 203 (2003).
[21]G. Y. Yang, J. M. Finder, J. Wang, Z. L. Wang, Z. Yu, J. Ramdani, R. Droopad, K. Eisenbeiser, and R. Ramesh, J. Mater. Res. **17**, 204 (2002).
[22]V. Vaithyanathan, J. Lettieri, J. H. Haeni, J. Schubert, L. Edge, W. Tian, and D. G. Schlom (unpublished).
[23]R. M. C. de Ameida and I. J. R. Baumvol, Surf. Sci. Rep. **49**, 1 (2003).
[24]V. Shutthanandan, S. Thevuthasan, Y. Liang, E. M. Adams, Z. Yu, and R. Droopad, Appl. Phys. Lett. **80**, 1803 (2002).
[25]W. K. Chu, J. W. Mayer, and M. A. Nicolet, *Backscattering Spectroscopy* (Academic, New York, 1978).
[26]J. Lettieri, J. H. Haeni, and D. G. Schlom, J. Vac. Sci. Technol. A **20**, 1332 (2002).
[27]C. D. Theis and D. G. Schlom, J. Vac. Sci. Technol. A **14**, 2677 (1996).
[28]1 ML is defined as the concentration of atoms on the (001) surface of silicon, i.e., 6.78×10^{14} at./cm^2.
[29]Y. Liang, S. Gan, and M. Engelhard, Appl. Phys. Lett. **79**, 3591 (2001).
[30]K. Iijima, T. Terashima, Y. Bando, K. Kamigaki, and H. Terauchi, J. Appl. Phys. **72**, 2840 (1992).
[31]A. Y. Cho, Surf. Sci. **17**, 494 (1969).
[32]W. H. Schulte, B. W. Busch, E. Garfunkel, T. Gustafsson, G. Schiwietz, and P. L. Grande, Nucl. Instrum. Methods Phys. Res. B **1883**, 16 (2001).
[33]R. M. Tromp, M. Copel, M. C. Reuter, M. Horn von Hoegen, J. Speidell, and R. Koudijs, Rev. Sci. Instrum. **62**, 2679 (1991).
[34]J. Q. He, C. L. Jia, V. Vaithyanathan, D. G. Schlom, J. Schubert, A. Gerber, H. H. Kohlstedt, and R. H. Wang, J. Appl. Phys. **97**, 104921 (2005).
[35]J. Shin, S. V. Kalinin, H. N. Lee, H. M. Christen, R. G. Moore, E. W. Plummer, and A. P. Baddorf, Surf. Sci. **581**, 118 (2005).
[36]M. Copel, E. Cartier, E. P. Gusev, S. Guha, N. Bojarczuk, and M. Poppeller, Appl. Phys. Lett. **78**, 2670 (2001).
[37]S. W. Jiang, Q. Y. Zhang, Y. R. Li, Y. Zhang, X. F. Sun, and B. Jiang, J. Cryst. Growth **274**, 500 (2005).